New K isomers in the neutron-rich N=100 isotones ^{162}Sm, ^{163}Eu, and ^{164}Gd

R. Yokoyama *et al.*

Phys. Rev. C **95**, 034313 — Published 15 March 2017

DOI: 10.1103/PhysRevC.95.034313

New K isomers in the neutron-rich $N = 100$ isotones, ^{162}Sm, ^{163}Eu, and ^{164}Gd

R. Yokoyama,[1,*] S. Go,[1] D. Kameda,[2] T. Kubo,[2] N. Inabe,[2] N. Fukuda,[2] H. Takeda,[2] H. Suzuki,[2] K. Yoshida,[2] K. Kusaka,[2] K. Tanaka,[2] Y. Yanagisawa,[2] M. Ohtake,[2] H. Sato,[2] Y. Shimizu,[2] H. Baba,[2] M. Kurokawa,[2] D. Nishimura,[3] T. Ohnishi,[2] N. Iwasa,[4] A. Chiba,[4] T. Yamada,[4] E. Ideguchi,[1] T. Fujii,[1] H. Nishibata,[5] K. Ieki,[6] D. Murai,[6] S. Momota,[7] Y. Sato,[8] J. W. Hwang,[8] S. Kim,[8] O. B. Tarasov,[9] D. J. Morrissey,[9] B. M. Sherrill,[9] G. Simpson,[10] and C. R. Praharaj[11]

[1] *Center for Nuclear Study, the University of Tokyo, 2-1 Hirosawa, Wako, Saitama 351-0198, Japan*
[2] *RIKEN, Nishina Center, 2-1 Hirosawa, Wako, Saitama 351-0198, Japan*
[3] *Department of Physics, Tokyo University of Science, 2641 Yamazaki, Noda, Chiba 278-8510, Japan*
[4] *Department of Physics, Tohoku University,6-3, Aramaki-aza-aoba, Aoba, Sendai, Miyagi 980-8578, Japan*
[5] *Department of Physics, Osaka University, 1-1 machikaneyama, Toyonaka, Osaka 560-0043, Japan*
[6] *Department of Physics, Rikkyo University, 3-34-1 Nishi-Ikebukuro, Toshima-ku, Tokyo 171-8501, Japan*
[7] *School of Environmental Science and Engineering, Kochi University of Technology, 185 Miyanokuchi, Tosayamada, Kami-city, Kochi 782-8502, Japan*
[8] *Department of Physics and Astronomy, Seoul National University, 1 Gwanak-ro, Gwanak-gu, Seoul 08826, Republic of Korea*
[9] *National Superconducting Cyclotron Laboratory (NSCL), Michigan State University (MSU), 640 South Shaw Lane, East Lansing, Michigan 48824-1321, U.S.A.*
[10] *LPSC, 53, Rue des Martyrs, F-38026 Grenoble Cedex, France*
[11] *Institute of Physiscs, Bhubaneswar 751005, India*

(Dated: February 17, 2017)

Very neutron-rich $Z \sim 60$ isotopes produced by in-flight fission of 345 MeV/nucleon ^{238}U beam at the RI Beam Factory, RIKEN Nishina Center have been studied by delayed γ-ray spectroscopy. New isomers are discovered in the neutron-rich $N = 100$ isotones, ^{162}Sm, ^{163}Eu, and ^{164}Gd. Half-lives, γ-ray energies and relative intensities of these isomers were obtained. Level schemes were proposed for these nuclei and the first 2^+ and 4^+ states were assigned for the even-even nuclei. The first 2^+ and 4^+ state energies decrease as the proton numbers get smaller. The energies and the half-lives of the new isomers are very similar to those of 4^- isomers known in less neutron-rich $N = 100$ isotones, ^{168}Er and ^{170}Yb. A deformed Hartree-Fock with angular momentum projection model suggests $K^\pi = 4^-$ two quasi-particle states with $\nu 7/2[633] \otimes \nu 1/2[521]$ configurations with similar excitation energy. The results suggest that neutron-rich $N = 100$ nuclei are well deformed and the deformation gets larger as Z decreases to 62. The onset of K isomers with the same configuration at almost the same energy in $N = 100$ isotones indicates that the neutron single-particle structures of neutron-rich isotones down to $Z = 62$ do not change significantly from those of the $Z = 70$ stable nuclei. Systematics of the excitation energies of new isomers can be explained without the predicted $N = 100$ shell gap.

PACS numbers: 23.35.+g

I. INTRODUCTION

Exploration of neutron-rich nuclei far from the line of β stability is attracting more and more interest. As experimental studies on unstable nuclei progressed, it was seen that nuclear structure of neutron-rich nuclei can be different from what is known in stable nuclei. One example is the appearance of new magic numbers at $N = 16$ or 34 [1, 2]. Appearance of such new phenomena shows the importance of the studies of nuclei far from stability.

Studies of unstable nuclei are being extended to heavier mass regions with the advent of new facilities. In the neutron-rich rare-earth region, a new deformed shell gap is predicted at $N = 100$ [3, 4]. Due to the deformed shell gap, $N = 100$ nuclei may have additional stability compared to neighboring isotopes. Deformed configurations and band structures in the rare-earth region have been studied using mean-field or Hartree-Fock models [5, 6]. Rare-earth nuclei with $N \geq 90$ are known to be well deformed. This can be seen from the systematics of excitation energies of the first 2^+ states of even-even nuclei, which get as low as ∼100 keV in $N \geq 90$ nuclides as shown in Fig.1 of Ref. [7]. A shape transition from spherical to prolate-deformed ground-state shape occurs when going from $N = 88$ to 90. The quadrupole deformation is expected to be largest at around the midshell region, $Z \sim 66$, $N \sim 104$ [8–10]. In order to examine how the deformation evolves in neutron-rich rare-earth nuclei and to confirm the existence of a shell gap at $N = 100$, measurements of the excited states are a possible method to probe these properties. Systematics of the moment of inertia obtained from the excitation energies of the ground-state band will give us a picture of nuclear shape evolution. Measurements of excited states will also give us useful information to understand the deformed single-

* yokoyama@cns.s.u-tokyo.ac.jp

particle structure around $N = 100$.

Nuclear deformation of neutron-rich rare-earth nuclei is of great importance also from an astrophysical point of view since it is supposed to have a significant influence on the r-process abundances. The r-process, or rapid neutron capture process, occurs at a fast rate compared to β decays [11] and is responsible for the synthesis of roughly half the $Z > 26$ nuclei in the universe. There are distinct peaks in r-process mass abundances at $A \sim 80$, 130 and 195. The origin of those peaks was pointed out to be the neutron closed shells [11]. There is a smaller peak in the r-process abundance at $A \sim 160$ known as the rare-earth element peak. Surman *et al.* hypothesized that the interplay of nuclear deformation and β decay was responsible for the formation of the rare-earth peak [12, 13]. They argue that the formation of the rare-earth peak does not occur in the steady phase of the r-process but at a later time of the process as the free neutrons disappear. Recent theoretical studies on such late-time r-process dynamics [14, 15] point to the importance of nuclear properties such as masses, β-decay rates or neutron capture rates of neutron-rich rare-earth nuclei for the formation of the rare-earth peak. Ghorui *et al.* [5] argue that the stability of $N = 100$ nuclei will make them serve as a waiting point in the nucleosynthesis of the r-process. Experimental studies of the deformation of this region will lead to important information for understanding the r-process abundances.

A spectroscopic study of $Z = 62$ (Sm) nuclei so far has been carried out by using spontaneous fission of ^{252}Cf [16]. Energies of the first 2^+ and 4^+ states suggest that the nuclei are deformed up to $N = 98$, but no data are available for $N = 100$. In deformed nuclei with axial symmetry, a transition between states with large differences of the K-quantum number is hindered and gives rise to K isomerism. $K^\pi = 4^-$ isomers are known in stable $N = 100$ nuclei, ^{168}Er and ^{170}Yb, and considered to be neutron two quasi-particle excitations [17, 18]. Isomers with similar excitations should be observed in the $N = 100$ isotones at lower proton numbers. Recently, the production of the high intensity beams of such neutron-rich isotopes became available at the Radioactive Isotope Beam Factory (RIBF) in RIKEN Nishina Center by in-flight fission of the ^{238}U beam. A couple of quasi-particle K isomers have been reported in rare-earth nuclei with $N = 98$ and 102 at RIBF [19, 20]. Isomer spectroscopy on the $N = 100$ nuclei is expected to give us information related to nuclear deformations and single-particle structures through the excitation energies of isomers or ground-state bands.

II. EXPERIMENT AND ANALYSIS

The neutron-rich $Z \sim 60$ nuclei were produced by in-flight fission of 345 MeV/nucleon ^{238}U beam at the RIBF. The fission fragments were separated and identified in the BigRIPS in-flight separator [21]. Measurements were performed with two different separator settings. One centered on $Z = 64$ nuclei and the other on $Z = 59$ nuclei. The primary ^{238}U beam bombarded a production target (made of Be 4.93-mm thick for higher Z setting, and 3.96-mm thick for lower the Z setting). The average intensity of the primary ^{238}U^{86+} beam was 0.24 pnA for the lower Z setting and 0.31 pnA for the higher Z setting, respectively. The produced RI beams were identified event-by-event by their proton numbers (Z) and mass-to-charge ratio (A/Q). These quantities were obtained by the measurement of the magnetic rigidity ($B\rho$), time of flight (TOF), and energy loss (ΔE) in BigRIPS. The TOF was obtained from the time difference between plastic scintillation counters at achromatic foci called F3 and F7 located at the beginning and the end of the second stage of the BigRIPS, respectively. A detailed explanation of the particle identification at the BigRIPS is found in Ref. [22]. In addition, a Si stack detector was installed in the final focal plane, F12. It consisted of 14 layers of Si detectors for the measurement of ΔE and total kinetic energies (E) of beam ions. It was designed to stop all ions of interest. As a tracker of the implanted ions, two PPACs (Parallel Plate Avalanche Counters) were installed before the Si stack detector in order to deduce the implantation position.

The γ rays from the ions stopped at F12 were detected by four clover-type high-purity Ge detectors placed around the Si stack detector. The total detection efficiency for 1333-keV photons emitted from the center of the Clover array was ∼2.5%. The energies and times of delayed γ rays detected within a time window of 30 μs following the implantation of the beam were recorded. The time of flight between the production target and the F12 focus was ∼550 ns for ^{168}Gd. Therefore, the half-life of the observable isomers was limited to between ∼100 ns and ∼30 μs in this measurement.

In order to search for new isomers, energy spectra of delayed γ rays from each isotope were examined by gating on the RI particle identification (PID) obtained from the A/Q and Z values. For each isotope, energies, half-lives, and relative intensities of the γ rays were obtained. Half-lives are obtained by likelihood fitting of a time spectrum between beam implantation and γ-ray emission with a function with an exponential decay and a constant background. Relative intensities of the γ rays were obtained for the isotopes. The detection efficiencies of γ rays were estimated for each isotope by a Monte Carlo simulation using Geant4 [23, 24] by taking the position distribution of the beam implantation into account. The consistency of our analysis of relative intensities was confirmed by using known γ rays in less neutron-rich isotopes.

III. RESULTS

In this experiment, three new isomers were systematically observed in the $N = 100$ isotones, ^{162}Sm, ^{163}Eu, and ^{164}Gd. Energy spectra of the delayed γ rays from

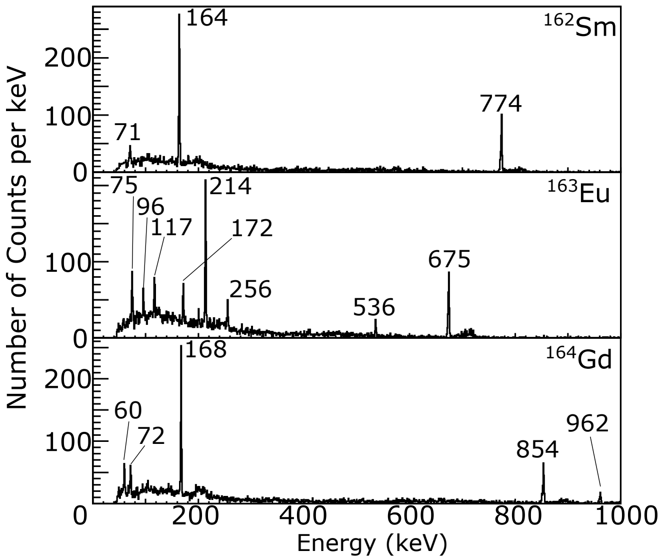

FIG. 1. Delayed γ-ray spectra for the new $N = 100$ isomers. The numbers labeling the peaks show γ-ray energies in keV. All the peaks with labels are identified and shown in the level schemes in Fig. 3. The time window is gated up to 10 μs for ^{162}Sm, 6 μs for ^{163}Eu and 4 μs for ^{164}Gd. Times close to the beam implantation (<100 to 400 ns, energy dependent) were excluded from the window in order to avoid prompt γ rays or X rays.

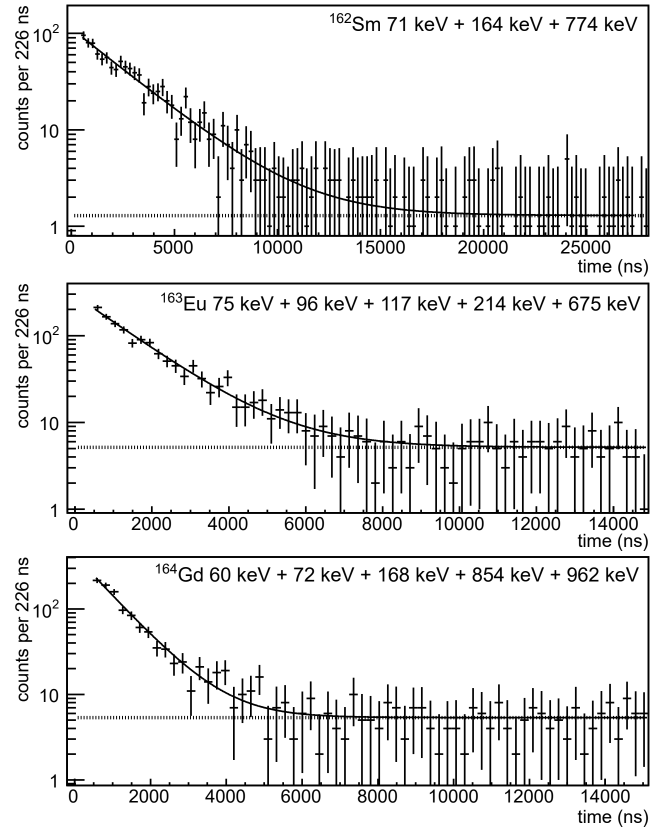

FIG. 2. Summed time spectra for the γ decays of new $N = 100$ isomers. The fits with an exponential decay and a constant background are shown as solid curves. The dashed lines represent a constant component of the fitting function.

the new isomers are shown in Fig. 1. Time spectra for each isomer decay are shown in Fig. 2. The γ-ray energies, relative intensities and half-lives of each isotope are listed in Table I. Level schemes were constructed for the three nuclei as shown in Fig. 3.

A. ^{162}Sm

The two peaks in the spectrum of ^{162}Sm at 71.0 and 164.3 keV were assigned as the γ rays from $2^+ \to 0^+$ and $4^+ \to 2^+$ members of the ground-state band which follows the systematic trend of the transition energies of the less neutron-rich Sm isotopes, ^{158}Sm and ^{160}Sm as shown in [16]. The 774.1-keV γ ray is assumed to be the transition decaying from the isomeric state to the 4^+ state of the ground-state band. The isomer in ^{162}Sm was assigned to decay by a single cascade since the relative intensities of the three γ rays after the correction of internal conversion [25] agreed with each other. This indicates that there is no branching in the decay. The spin of the isomeric state of ^{162}Sm was assigned as 4 because only one decay was observed from the isomer to the $J = 4$ level of the ground-state band. For other spin assignments, isomeric decays to states with spins other than 4 should be observed. For example, there are $K^\pi = 5^-$ isomers known in ^{156}Sm, ^{158}Sm, and ^{160}Sm [16]. However, a $J^\pi = 5^-$ assignment was excluded since the $5^- \to 6^+$ γ ray (~ 510 keV) was not observed. The isomeric state of ^{162}Sm can be interpreted as the

TABLE I. List of γ-ray energies, half-lives, proposed multipolarity and relative intensities of new isomers obtained in this study. The relative intensity I_{γ_rel} is the ratio of the number of emitted γ-rays normalized by the most intense one in a nuclide. I_{γ_rel} does not include the correction of the internal conversion.

nuclide	$T_{1/2}$ (μs)	E_γ (keV)	Mult.	I_{γ_rel} (%)
^{162}Sm	1.78(7)	71.0	E2	9.8(1.6)
		164.3	E2	62(3)
		774.1	E1	100(7)
^{163}Eu	0.869(29)	74.9	M1	18(3)
		96.2	M1	7.8(2.2)
		117.1	M1	15(3)
		171.9	E2	19(3)
		214.1	E2	66(5)
		256.1	E1	9(3)
		536.2	M1	14(4)
		674.9	E1	100(9)
^{164}Gd	0.580(23)	60.2	E1	14(3)
		72.0	E2	19(4)
		168.0	E2	71(5)
		854.1	E1	100(11)
		961.9	M1	37(7)

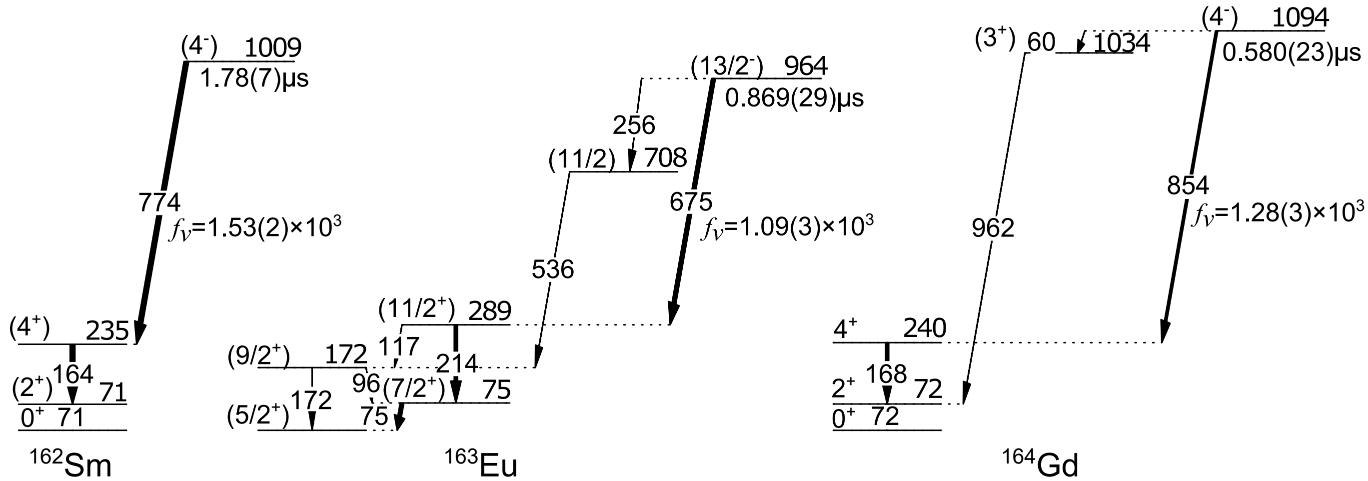

FIG. 3. Proposed level schemes of ^{162}Sm, ^{163}Eu, and ^{164}Gd obtained in this work. Energies of each level and γ ray are labeled in keV. Half-lives are shown below the isomeric states. Widths of the arrows are proportional to the intensities of each decay. Reduced hindrance factors, f_ν (see text), of the decays from the isomeric states to the ground-state bands assuming E1 transitions are shown.

same configuration as known isomers with $K^\pi = 4^-$ in $N = 100$ isotones, ^{168}Er and ^{170}Yb [17, 18]. The isomers of ^{168}Er and ^{170}Yb decay by E1 transitions to the $J^\pi = 4^+$ level of the ground-state band. The reduced hindrance factor, f_ν, of the E1 transitions in ^{168}Er and ^{170}Yb are 1.4×10^3 and 1.2×10^3, respectively, where $f_\nu = F_W^{1/\nu}$, $F_W = T_{1/2\_\mathrm{exp.}}/T_{1/2\_\mathrm{Weisskopf}}$, and $\nu = \Delta K - \lambda$. The hindrance factor obtained for ^{162}Sm in this work by assuming an E1 decay was $1.53(2)\times10^3$, which is consistent with the cases in ^{168}Er or ^{170}Yb. It supports the $J^\pi = 4^-$ assignment of the isomer in ^{162}Sm and its decay by a hindered E1.

B. ^{164}Gd

The 72.0- and 168.0-keV γ rays in ^{164}Gd were reported as the $2^+ \to 0^+$ and $4^+ \to 2^+$ transitions of the ground-state band in Ref. [26]. In this work, new delayed γ rays were observed at 60.2, 854.1, and 961.9 keV. The isomeric state was assigned at 1094.1 keV since the energy sums of the 60.2-, 961.9-, 854.1-, and 168.0-keV γ rays were in good agreement. Relative intensities of the γ rays were also consistent with the proposed level scheme. The spin and parity of the isomeric state at 1094.1 keV was tentatively assigned as 4^- by using the same arguments as those in the analysis of ^{162}Sm. The reduced hindrance factor of the 854.1-keV isomeric decay of ^{164}Gd obtained in this work was $1.28(3) \times 10^3$. The 60.2-keV transition from the isomeric state was assigned as an E1 transition since the intensity conservation between 60.2- and 961.9-keV decays matches with this multipolarity assignment the best. The known isomer in ^{168}Er has a decay branch to the $J^\pi = 3^+$ state of the $K^\pi = 2^+$ γ-vibrational band at 896 keV. Assuming that the spin and parity of the isomeric state is 4^- and the 60.2-keV decay is an E1 transition, $J^\pi = 3^+$ is the best candidate for the 1034-keV state in ^{164}Gd. The inverse order of the placement of 60.2- and 961.9-keV γ rays cannot be excluded. If the 60.2-keV decay is placed below the 961.9-keV decay, there should be a state at 132 keV instead of 1034 keV. This is also possible but less probable from the level systematics. The excited state at 132 keV should have negative parity since the 60.2-keV transition is E1. However, no negative-parity state is known below the 4^- isomer at 1094 keV in ^{168}Er.

In ^{168}Er, a decay from a $K^\pi = 4^-$ isomer to a $J^\pi = 3^+$ state of a $K^\pi = 2^+$ γ-vibrational band has been observed [27]. Such $K^\pi = 2^+$ bands are also known in other $N = 100$ isotones, ^{166}Dy and ^{170}Yb. The 1034-keV state in ^{164}Gd can also be a member of the γ-vibrational band. The reduced hindrance factor of the decay from 4^- isomer to the proposed 3^+ state of ^{164}Gd is $2.37(10) \times 10^6$, which is similar in strength to that of ^{168}Er, 5.2×10^6. The intra-band transition from the 3^+ state to the second 2^+ state is expected to have an energy less than 100 keV, from a comparison with those in ^{168}Er. The intensity should be much weaker than the decay to the first 2^+ state of the ground band. The 3^+ state was not observed in ^{162}Sm probably because its energy is either higher or almost the same as that of the isomeric state.

C. ^{163}Eu

In ^{163}Eu, 8 delayed transitions were newly observed in this work. The ground state of ^{163}Eu was tentatively assigned to be $5/2^+$ from the systematics [28]. The ground-state band was identified up to the 289-keV $(11/2^+)$ state. The energies of these states agree well with the systematics of the less neutron-rich Eu isotopes, ^{157}Eu and ^{159}Eu [29]. The energy sums of $\Delta J = 1$ γ cascades

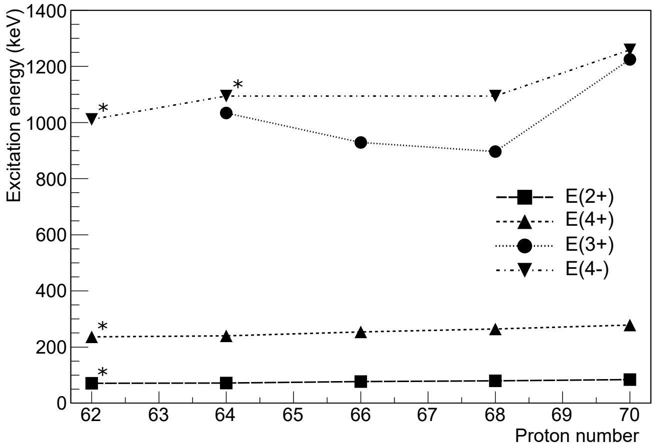

FIG. 4. Systematics of the excitation energies of the states in even-even $N = 100$ isotones. The $J^\pi = 4^+$ state of the ground-band, $J^\pi = 3^+$ state of $K^\pi = 2^+$ γ band, and $K^\pi = 4^-$ isomeric states are shown. Symbols with an asterisk represent the data points newly obtained in this work. The levels of ^{170}Yb, ^{168}Er, ^{166}Dy, and ^{164}Gd are from [17], [18], [30], and [26], respectively.

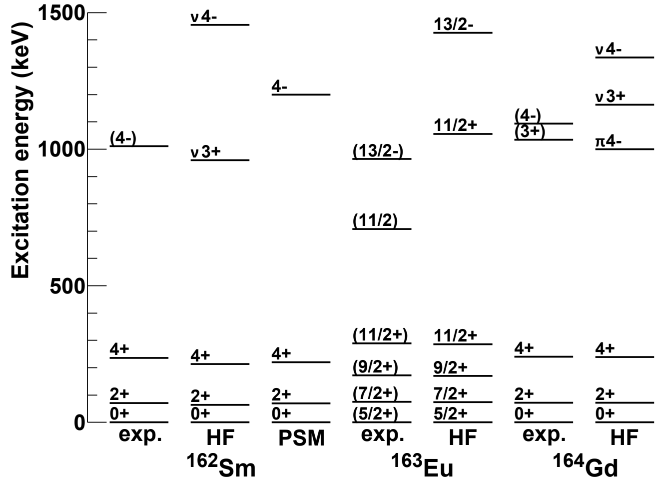

FIG. 5. Measured and theoretical values of excitation energies for ^{162}Sm, ^{163}Eu, and ^{164}Gd. Deformed Hartree-Fock calculations were performed on ^{162}Sm and ^{164}Gd and the results are shown with the labels, "HF". The levels with neutron quasiparticle excitations are labeled as νJ^π and those with proton excitations are labeled as πJ^π A prediction by a Projected Shell Model calculation for ^{162}Sm [31] is labeled "PSM" in the figure. For the theoretical calculations, only the lowest J state (band-head) of each band is shown.

agree well with those of the crossover $\Delta J = 2$ decays. The isomeric state was assigned at 963.9 keV and decays to both the 289.0- and 708.1-keV states. This scheme was deduced from the agreement of the energy sum of the 536.2- and 256.1-keV γ rays with that of the 117.1- and 674.9-keV transitions. The spin and parity of the isomeric state was assigned as $(13/2^-)$ from the decay pattern and systematics of the hindrance. The isomeric state decays only to the $(11/2^+)$ state of the ground-state band. In the case of a spin assignment other than 13/2, a decay to other members of the ground-state band should be observed. The isomer of ^{163}Eu can be interpreted as the coupling of the $K^\pi = 4^-$ neutron excitation and the $\pi 5/2[413]$ odd proton. The reduced hindrance factor of the 674.9-keV decay in ^{163}Eu was $1.09(3) \times 10^3$ which is similar to those of the isomers in the even-even $N = 100$ nuclei. The spin of the 708-keV state was assigned as 11/2 since it decays to a $9/2^+$ member of the ground-state band. The opposite placement of the 256.1- and 536.2-keV decays is also possible in ^{163}Eu. The measured relative intensities of the γ rays were consistent with this level scheme assignment.

IV. DISCUSSIONS

In this work, the first 4^+ and 2^+ states have been observed for the first time in ^{162}Sm. The systematics of the 4^+ and 2^+ energies show a slight decrease as proton number decreases as shown in Fig. 4. All the nuclei in the figure have an $E(4^+)/E(2^+)$ ratio of $\sim$3.3, which indicates that the ground-state bands have rigid rotational character. Those results indicates that the nucleus is more deformed for lower Z isotones.

The 3^+ energy has a minimum at $Z = 68$ (Er) and gradually increases as proton number decreases. Trends of the γ vibrations from various experimental and theoretical data on rare-earth and actinide nuclei are summarized in [32]. The bandheads of $K^\pi = 2^+$ γ-vibrational bands become particularly lower in transitional regions between spherical and deformed shapes. The increase of the γ-band energy in Gd and Sm indicates that the nucleus becomes more rigidly deformed and is some distance away from the shape transitional region.

The two new isomers discovered in ^{162}Sm and ^{164}Gd have similar excitation energies and half-lives to those of the known 4^- isomers in ^{170}Yb and ^{168}Er. Figure 5 shows the comparison of the experimental and theoretical excitation energies. Projected Shell Model (PSM) [31] and Deformed Hartree-Fock (HF) model with angular momentum (J) projection [5, 33–35] were used to understand the structures of the states obtained in the experiment.

In the HF and J projection theory, the deformed Hartree-Fock equations are solved self-consistently using the residual interaction among nucleons to obtain the Hartree-Fock wave functions of the deformed orbits. The Hartree-Fock procedure is based on the variational principle for a many-particle system [36, 37] and gives a good account of the deformation properties and band structures of nuclei. It also correctly predicts the shapes and microscopic properties of light and heavy nuclei [36, 38, 39]. Assuming a ^{132}Sn core, the model space consists of the $3s_{1/2}$, $2d_{3/2}$, $2d_{5/2}$, $1g_{7/2}$, $1h_{9/2}$ and $1h_{11/2}$ proton space and $3p_{1/2}$, $3p_{3/2}$, $2f_{5/2}$, $2f_{7/2}$, $1h_{9/2}$, and

$1i_{13/2}$ neutron space. For example for ^{162}Sm, there are 12 protons and 18 neutrons in this active model space. A surface delta interaction is used as the residual interaction [5, 33–35]. The energy spectra and electromagnetic transitions are obtained by angular momentum projection from suitable intrinsic states based on the respective Hartree-Fock solutions. This model calculation showed substantial agreement for two quasi-particle excitations and their band structure for the $N = 90$ to 96 even-even Nd isotopes [5] and for many other nuclei [33, 34]. It predicts the systematics of the deformations in the rare-earth region quite well [5, 33].

Deformed Hartree-Fock calculations were performed for ^{162}Sm, ^{163}Eu, and ^{164}Gd. Deformation parameters were self-consistently obtained by the calculation, which were $\beta_2 = 0.33$ and $\beta_2 = 0.34$ for ^{162}Sm and ^{164}Gd, respectively. Properties of the calculated bandhead states are listed in Table II. Calculated magnetic moments of quasi-particle states reflect the assigned configurations in ^{162}Sm, ^{163}Eu, and ^{164}Gd.

TABLE II. Properties of isomers and bandheads from the HF calculation. Spectroscopic quadrupole moments at bandheads are in eb and magnetic moments are in nuclear magnetons. See [34] for definitions of Q_s and μ.

A	K^π	configuration	Q_s (in eb)	μ (in μ_N)
^{162}Sm	4^-	$\nu(1/2^- 7/2^+)$	3.037	22.03
	3^+	$\nu(1/2^- 5/2^-)$	3.116	24.18
^{163}Eu	$5/2^+$	$\pi 5/2^+$	-2.201	-29.26
	$11/2^+$	$\pi 5/2^+ \nu(1/2^- 5/2^-)$	-3.658	-102.53
	$13/2^-$	$\pi 5/2^+ \nu(1/2^- 7/2^+)$	-3.974	-135.489
^{164}Gd	4^-	$\nu(1/2^- 7/2^+)$	3.20	21.84
	3^+	$\nu(1/2^- 5/2^-)$	2.594	12.14

A. ^{164}Gd

In the Deformed HF calculation, $K^\pi = 4^-$ states with two quasi-particle excitations with the configuration of $\nu 7/2[633] \otimes \nu 1/2[521]$ and $\pi 3/2[411] \otimes \pi 5/2[532]$ appear at 1336 and 1000 keV above the ground state, respectively. In the $\pi 4^-(5/2^- 3/2^+)$ case, the $5/2^-$ deformed orbit has contribution from the $h_{9/2}$ proton and connects it by an E1 decay to the $g_{7/2}$ component of the $3/2^+$ deformed orbit. In contrast the E1 matrix element of the $\nu 4^-$ state decay to the ground band is much smaller and it is an 0.58-μs isomer. The faster E1 transition of the $\pi 4^-$ bandhead remains undetected in the present experiment where we cannot detect isomers with half-life smaller than 100 nano-seconds. Of the two $K^\pi = 4^-$ configurations of ^{164}Gd, the interaction matrix element connecting the two configurations is very small and there is negligible mixing between these two bands.

B. ^{162}Sm

In the case of ^{162}Sm, a $K^\pi = 4^-$ state with the configuration of $\nu 7/2[633] \otimes \nu 1/2[521]$ appears at 1455 keV above the ground state in the Deformed HF calculation. The $\nu 3^+$ state of ^{162}Sm appearing in the HF calculation can quickly decay to the ground band via a $\Delta K = 3$ transition and is not detected as an isomer in this measurement. Because the intensities are almost conserved in the cascade below the 4^- isomer, the 3^+ two quasi-particle state must lie either above, or be quasi-degenerate with, the 4^- isomer and was not observed.

The Projected Shell Model (PSM) calculation in Ref. [31] also predicts the $K^\pi = 4^-$ state at 1.2 MeV above the ground state in ^{162}Sm. This calculation reproduces the excitation energies of isomers in ^{156}Sm and ^{158}Sm very well [31]. The PSM calculation also reproduces the 4^- state at low energy in ^{162}Sm. In this calculation the deformation parameter $\beta_2 = 0.319$ was used as input.

The hindrance factors of the new isomers, $f_\nu \sim 10^3$ for E1 transitions with $\Delta K = 4$, agree with the systematics of the similar decays of deformed nuclei with $A > 100$ given in Ref. [40]. Such a high hindrance of the γ decay suggests that the purity of the K-quantum number is high in this configuration. The existence of the isomers with such high K-hindrance shows that the nucleus is well deformed with good axial symmetry. The trends of the ground-state bands and γ-vibrational bands indicate that the prolate deformation of the $N = 100$ nuclei is getting larger and more rigid as the proton number decreases down to ^{162}Sm. It raises the necessity of further investigations of lower Z nuclei for locating the deformation maximum in the rare-earth region that may have a significant influence on r-process abundances.

From the experimental result that the excitation energies and the hindrance factors of $K^\pi = 4^-$ isomers are very close to each other among $N = 100$ isotones, the deformed single-particle levels at the $N = 100$ neutron Fermi surface is expected to be stable against the change of proton numbers. This indicates that there is no significant change of the single-particle structure of neutrons for the $62 \leq Z \leq 70$ isotones at $N = 100$. If the shell gap at $N = 100$ appears in $Z \sim 62$ nuclei [3, 4], single-particle levels should be affected and would change the excitation energy of the $K^\pi = 4^-$ isomer when going from $Z = 62$ to 70. According to the HF calculation, the $\nu 1/2[521]$ and $\nu 7/2[633]$ orbitals are located below and above the $N = 100$ Fermi surface and the excitation energy of the isomer is expected to become higher as the deformed shell gap appears. However, no significant change has been observed in the excitation energy of the $K^\pi = 4^-$ isomer between $Z = 62$ and 68, while the local maximum of the $E(2^+)$ systematics becomes more distinct in $Z = 62$ isotopes than in $Z = 68$ [19]. The systematics of the isomeric state do not prove the existence of a $N = 100$ shell gap. There is no experimental mass data available for the Sm or Gd isotopes in the AME2012 compilation [41] to check the stability at $N = 100$ but at least for the Yb isotopes, no kink in the structure can be seen at $N = 100$ in the mass data. The local maximum of $E(2^+)$ does not necessarily reflect the shell gap directly and may be caused by other reasons. In order to confirm the predicted shell gap at $N = 100$ in [3, 4], further studies such as mass measurements should be performed.

V. CONCLUSIONS

New isomers with μs half-lives were discovered in the neutron-rich $N = 100$ isotones, ^{162}Sm, ^{163}Eu, and ^{164}Gd. Level schemes of these nuclei were constructed. The isomers of ^{162}Sm and ^{164}Gd were assigned as 4^-. By comparing with a Deformed HF and J Projection Model and Projected Shell Model calculations, the isomeric states can be interpreted as having a $\nu 7/2[633] \otimes \nu 1/2[521]$ configuration, the same configuration as other $N = 100$ 4^- isomers known in ^{168}Er and ^{170}Yb. The isomeric state of ^{163}Eu can be interpreted as a coupling of the $\nu 7/2[633] \otimes \nu 1/2[521]$ and the $\pi 5/2[413]$ configuration. The existence of the K isomer and the trends of excitation energies indicate the nucleus is well deformed with axial symmetry. Observation of the 4^- isomer at almost the same energy in the $62 \leq Z \leq 70$ isotones suggests that the neutron single-particle shell structures around the $N = 100$ Fermi surface in neutron-rich nuclei down to $Z = 62$ does not change significantly from those at stability. Systematics of the excitation energies of new isomers can be explained without the predicted $N = 100$ shell gap. The results of this study will contribute to the further understanding of nuclear deformation and single-particle structure in neutron-rich rare-earth nuclei and consequently provide input to the calculation of r-process abundances. It also provides motivation for the study of neutron-rich rare-earth nuclei beyond $N = 100$.

ACKNOWLEDGMENTS

VI. ACKNOWLEDGMENT

The present experiment was carried out at the RI Beam Factory operated by RIKEN Nishina Center, RIKEN and CNS, University of Tokyo. The authors are grateful to the RIBF accelerator crew for providing us with the uranium beam. They also would like to thank Dr. Y. Yano, RIKEN Nishina Center, for his support and encouragement. The authors O.T., D.M., and B.S. were supported by the US National Science Foundation under Grant No. PHY-11-02511. The author R.Y. was supported by ALPS program by the University of Tokyo and as JSPS fellow No. JP15J10788. Work of C.R.P. was supported by SERB Project SB/S2/HEP-06/2013.

[1] A. Ozawa, T. Kobayashi, T. Suzuki, K. Yoshida, and I. Tanihata, Physical Review Letters **84**, 5493 (2000).

[2] D. Steppenbeck, S. Takeuchi, N. Aoi, P. Doornenbal, M. Matsushita, H. Wang, H. Baba, N. Fukuda, S. Go, M. Honma, J. Lee, K. Matsui, S. Michimasa, T. Motobayashi, D. Nishimura, T. Otsuka, H. Sakurai, Y. Shiga, P.-a. Söderström, T. Sumikama, H. Suzuki, R. Taniuchi, Y. Utsuno, J. J. Valiente-Dobón, and K. Yoneda, Nature **502**, 207 (2013).

[3] L. Satpathy and S. K. Patra, Nuclear Physics A **722**, 24c (2003).

[4] L. Satpathy and S. K. Patra, Journal of Physics G: Nuclear and Particle Physics **30**, 771 (2004).

[5] S. K. Ghorui, P. K. Raina, P. K. Rath, A. K. Singh, Z. Naik, S. K. Patra, and C. R. Praharaj, International Journal of Modern Physics E **21**, 1250070 (2012).

[6] S. K. Ghorui, B. B. Sahu, C. R. Praharaj, and S. K. Patra, Physical Review C **85**, 064327 (2012).

[7] R. F. Casten, D. D. Warner, D. S. Brenner, and R. L. Gill, Physical Review Letters **47**, 1433 (1981).

[8] P. Möller, J. R. Nix, W. D. Myers, and W. J. Swiatecki, Atomic Data and Nuclear Data Tables **59**, 185 (1995).

[9] G. A. Lalazissis, S. Raman, and P. Ring, Atomic Data and Nuclear Data Tables **71**, 1 (1999).

[10] S. Hilaire and M. Girod, The European Physical Journal A **33**, 237 (2007).

[11] E. M. Burbidge, G. R. Burbidge, W. A. Fowler, and F. Hoyle, Reviews of Modern Physics **29**, 547 (1957).

[12] R. Surman, J. Engel, J. R. Bennett, and B. S. Meyer, Physical Review Letters **79**, 1809 (1997).

[13] R. Surman and J. Engel, Physical Review C **64**, 035801 (2001), arXiv:0103049 [nucl-th].

[14] M. R. Mumpower, G. C. McLaughlin, and R. Surman, Physical Review C **85**, 045801 (2012), arXiv:1109.3613.

[15] M. R. Mumpower, G. C. McLaughlin, and R. Surman, Physical Review C **86**, 035803 (2012), arXiv:1204.0437.

[16] G. S. Simpson, W. Urban, J. Genevey, R. Orlandi, J. A. Pinston, A. Scherillo, A. G. Smith, J. F. Smith, I. Ahmad, and J. P. Greene, Physical Review C **80**, 024304 (2009).

[17] C. Y. Wu, D. Cline, M. W. Simon, R. Teng, K. Vetter, M. P. Carpenter, R. V. F. Janssens, and I. Wiedenhöver, Physical Review C **68**, 044305 (2003).

[18] P. M. Walker, W. H. Bentley, S. R. Faber, R. M. Ronningen, R. B. Firestone, F. M. Bernthal, J. Borggreen, J. Pedersen, and G. Sletten, Nuclear Physics A **365**, 61 (1981).

[19] Z. Patel, P.-A. Söderström, Z. Podolyák, P. H. Regan, P. M. Walker, H. Watanabe, E. Ideguchi, G. S. Simpson, H. L. Liu, S. Nishimura, Q. Wu, F. R. Xu, F. Browne, P. Doornenbal, G. Lorusso, S. Rice, L. Sinclair, T. Sumikama, J. Wu, Z. Y. Xu, N. Aoi, H. Baba,

F. L. Bello Garrote, G. Benzoni, R. Daido, Y. Fang, N. Fukuda, G. Gey, S. Go, A. Gottardo, N. Inabe, T. Isobe, D. Kameda, K. Kobayashi, M. Kobayashi, T. Komatsubara, I. Kojouharov, T. Kubo, N. Kurz, I. Kuti, Z. Li, M. Matsushita, S. Michimasa, C.-B. Moon, H. Nishibata, I. Nishizuka, A. Odahara, E. Şahin, H. Sakurai, H. Schaffner, H. Suzuki, H. Takeda, M. Tanaka, J. Taprogge, Z. Vajta, A. Yagi, and R. Yokoyama, Physical Review Letters **113**, 262502 (2014).

[20] Z. Patel, Z. Podolyák, P. M. Walker, P. H. Regan, P. A. Söderström, H. Watanabe, E. Ideguchi, G. S. Simpson, S. Nishimura, F. Browne, P. Doornenbal, G. Lorusso, S. Rice, L. Sinclair, T. Sumikama, J. Wu, Z. Y. Xu, N. Aoi, H. Baba, F. L. Bello Garrote, G. Benzoni, R. Daido, Z. Dombrádi, Y. Fang, N. Fukuda, G. Gey, S. Go, A. Gottardo, N. Inabe, T. Isobe, D. Kameda, K. Kobayashi, M. Kobayashi, T. Komatsubara, I. Kojouharov, T. Kubo, N. Kurz, I. Kuti, Z. Li, H. L. Liu, M. Matsushita, S. Michimasa, C. B. Moon, H. Nishibata, I. Nishizuka, A. Odahara, E. Şahin, H. Sakurai, H. Schaffner, H. Suzuki, H. Takeda, M. Tanaka, J. Taprogge, Z. Vajta, F. R. Xu, A. Yagi, and R. Yokoyama, Physics Letters, Section B: Nuclear, Elementary Particle and High-Energy Physics **753**, 182 (2016).

[21] T. Kubo, Nuclear Instruments and Methods in Physics Research Section B: Beam Interactions with Materials and Atoms **204**, 97 (2003).

[22] T. Ohnishi, T. Kubo, K. Kusaka, A. Yoshida, K. Yoshida, M. Ohtake, N. Fukuda, H. Takeda, D. Kameda, K. Tanaka, N. Inabe, Y. Yanagisawa, Y. Gono, H. Watanabe, H. Otsu, H. Baba, T. Ichihara, Y. Yamaguchi, M. Takechi, S. Nishimura, H. Ueno, A. Yoshimi, H. Sakurai, T. Motobayashi, T. Nakao, Y. Mizoi, M. Matsushita, K. Ieki, N. Kobayashi, K. Tanaka, Y. Kawada, N. Tanaka, S. Deguchi, Y. Satou, Y. Kondo, T. Nakamura, K. Yoshinaga, C. Ishii, H. Yoshii, Y. Miyashita, N. Uematsu, Y. Shiraki, T. Sumikama, J. Chiba, E. Ideguchi, A. Saito, T. Yamaguchi, I. Hachiuma, T. Suzuki, T. Moriguchi, A. Ozawa, T. Ohtsubo, M. a. Famiano, H. Geissel, A. S. Nettleton, O. B. Tarasov, D. P. Bazin, B. M. Sherrill, S. L. Manikonda, and J. a. Nolen, Journal of the Physical Society of Japan **79**, 073201 (2010).

[23] S. Agostinelli, J. Allison, K. Amako, J. Apostolakis, H. Araujo, P. Arce, M. Asai, D. Axen, S. Banerjee, G. Barrand, F. Behner, L. Bellagamba, J. Boudreau, L. Broglia, A. Brunengo, H. Burkhardt, S. Chauvie, J. Chuma, R. Chytracek, G. Cooperman, G. Cosmo, P. Degtyarenko, A. Dell'Acqua, G. Depaola, D. Dietrich, R. Enami, A. Feliciello, C. Ferguson, H. Fesefeldt, G. Folger, F. Foppiano, A. Forti, S. Garelli, S. Giani, R. Giannitrapani, D. Gibin, J. Gómez Cadenas, I. González, G. Gracia Abril, G. Greeniaus, W. Greiner, V. Grichine, A. Grossheim, S. Guatelli, P. Gumplinger, R. Hamatsu, K. Hashimoto, H. Hasui, A. Heikkinen, A. Howard, V. Ivanchenko, A. Johnson, F. Jones, J. Kallenbach, N. Kanaya, M. Kawabata, Y. Kawabata, M. Kawaguti, S. Kelner, P. Kent, A. Kimura, T. Kodama, R. Kokoulin, M. Kossov, H. Kurashige, E. Lamanna, T. Lampén, V. Lara, V. Lefebure, F. Lei, M. Liendl, W. Lockman, F. Longo, S. Magni, M. Maire, E. Medernach, K. Minamimoto, P. Mora de Freitas, Y. Morita, K. Murakami, M. Nagamatu, R. Nartallo, P. Nieminen, T. Nishimura, K. Ohtsubo, M. Okamura, S. O'Neale, Y. Oohata, K. Paech, J. Perl, A. Pfeiffer, M. Pia, F. Ranjard, A. Rybin, S. Sadilov, E. Di Salvo, G. Santin, T. Sasaki, N. Savvas, Y. Sawada, S. Scherer, S. Sei, V. Sirotenko, D. Smith, N. Starkov, H. Stoecker, J. Sulkimo, M. Takahata, S. Tanaka, E. Tcherniaev, E. Safai Tehrani, M. Tropeano, P. Truscott, H. Uno, L. Urban, P. Urban, M. Verderi, A. Walkden, W. Wander, H. Weber, J. Wellisch, T. Wenaus, D. Williams, D. Wright, T. Yamada, H. Yoshida, and D. Zschiesche, Nuclear Instruments and Methods in Physics Research Section A: Accelerators, Spectrometers, Detectors and Associated Equipment **506**, 250 (2003).

[24] J. Allison, K. Amako, J. Apostolakis, H. Araujo, P. A. Dubois, M. Asai, G. Barrand, R. Capra, S. Chauvie, R. Chytracek, G. A. P. Cirrone, G. Cooperman, G. Cosmo, G. Cuttone, G. G. Daquino, M. Donszelmann, M. Dressel, G. Folger, F. Foppiano, J. Generowicz, V. Grichine, S. Guatelli, P. Gumplinger, A. Heikkinen, I. Hrivnacova, A. Howard, S. Incerti, V. Ivanchenko, T. Johnson, F. Jones, T. Koi, R. Kokoulin, M. Kossov, H. Kurashige, V. Lara, S. Larsson, F. Lei, O. Link, F. Longo, M. Maire, A. Mantero, B. Mascialino, I. Mclaren, P. M. Lorenzo, K. Minamimoto, K. Murakami, P. Nieminen, L. Pandola, S. Parlati, L. Peralta, J. Perl, A. Pfeiffer, M. G. Pia, A. Ribon, P. Rodrigues, G. Russo, S. Sadilov, G. Santin, T. Sasaki, D. Smith, N. Starkov, S. Tanaka, E. Tcherniaev, B. Tomé, A. Trindade, P. Truscott, L. Urban, M. Verderi, A. Walkden, J. P. Wellisch, D. C. Williams, D. Wright, and H. Yoshida, IEEE Transactions on Nuclear Science **53**, 270 (2006).

[25] T. Kibédi, T. Burrows, M. Trzhaskovskaya, P. Davidson, and C. Nestor, Nuclear Instruments and Methods in Physics Research Section A: Accelerators, Spectrometers, Detectors and Associated Equipment **589**, 202 (2008).

[26] E. F. Jones, J. H. Hamilton, P. M. Gore, A. V. Ramayya, J. K. Hwang, and A. P. DeLima, The European Physical Journal A **25**, 467 (2005).

[27] G. D. Dracoulis, G. J. Lane, F. G. Kondev, H. Watanabe, D. Seweryniak, S. Zhu, M. P. Carpenter, C. J. Chiara, R. V. F. Janssens, T. Lauritsen, C. J. Lister, E. A. McCutchan, and I. Stefanescu, Physical Review C **81**, 054313 (2010).

[28] G. Audi, O. Bersillon, J. Blachot, and A. Wapstra, Nuclear Physics A **729**, 3 (2003).

[29] D. G. Burke, G. Løvhøiden, and E. R. Flynn, Nuclear Physics A **318**, 77 (1979).

[30] M. Asai, K. Tsukada, S. Ichikawa, A. Osa, Y. Kojima, M. Shibata, H. Yamamoto, K. Kawade, N. Shinohara, Y. Nagame, H. Iimura, Y. Hatsukawa, and I. Nishinaka, Journal of the Physical Society of Japan **65**, 1135 (1996).

[31] Y.-C. Yang, Y. Sun, S.-J. Zhu, M. Guidry, and C.-L. Wu, Journal of Physics G: Nuclear and Particle Physics **37**, 085110 (2010).

[32] R. K. Sheline, Reviews of Modern Physics **32**, 1 (1960).

[33] C. R. Praharaj, S. K. Patra, R. K. Bhowmik, and Z. Naik, Journal of Physics Conference Series **312**, 092052 (2011).

[34] S. K. Ghorui, C. R. Praharaj, P. K. Raina, Z. Naik, and S. K. Patra, AIP Conference Proceedings **1609**, 135 (2014).

[35] A. Faessler, P. Plastino, and S. A. Moszkowski, Physical Review **156**, 1064 (1967).

[36] G. Ripka, *Advances in Nuclear Physiscs, vol.1*, edited by M. Baranger and E. Vogt (Springer, 1968) pp. 183–259.

[37] D. Thouless, *Quantum mechanics of Many-Body Systems* (Academic Press, 1972).

[38] C. Praharaj and S. Khadkikar, J. Phys. G Nucl. Phys. **6**, 241 (1980).

[39] A. K. Rath, C. R. Praharaj, and S. B. Khadkikar, Physical Review C **47**, 1990 (1993).

[40] F. Kondev, G. Dracoulis, and T. Kibédi, Atomic Data and Nuclear Data Tables **103-104**, 50 (2015).

[41] M. Wang, G. Audi, A. H. Wapstra, F. G. Kondev, M. MacCormick, X. Xu, and B. Pfeiffer, Chinese Physiscs C **1287**, 1603 (2012).